

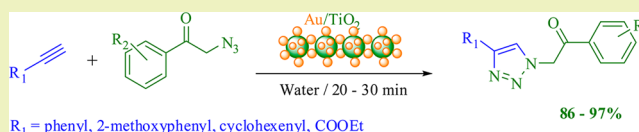
## Nanoporous Titania-Supported Gold Nanoparticle-Catalyzed Green Synthesis of 1,2,3-Triazoles in Aqueous Medium

Muthusamy Boominathan,<sup>†</sup> Nalenthiran Pugazhenthiran,<sup>‡</sup> Muthupandi Nagaraj,<sup>†</sup> Shanmugam Muthusubramanian,<sup>\*,†</sup> Sepperumal Murugesan,<sup>‡</sup> and Nattamai Bhuvanesh<sup>§</sup><sup>†</sup>Department of Organic Chemistry, <sup>‡</sup>Department of Inorganic Chemistry, School of Chemistry, Madurai Kamaraj University, Madurai 625 021, India<sup>§</sup>X-ray Diffraction Laboratory, Department of Chemistry, Texas A&M University, College Station, Texas 77842, United States

## S Supporting Information

**ABSTRACT:** Nanoporous titania-supported gold nanoparticles have been synthesized through the deposition–precipitation method, and the synthesized nanoparticles have been characterized by XRD, SEM, HRTEM, EDAX, BET adsorption isotherm, and IR and UV–vis spectral techniques. The efficiency of this catalyst toward green organic synthesis has been studied by carrying out the 1,3-dipolar cycloaddition of organic azides with a variety of terminal alkynes in water. The reaction proceeds regioselectively yielding the corresponding 1,4-disubstituted-1,2,3-triazole derivative in good to excellent yield.

**KEYWORDS:** Gold nanoparticles, Cycloaddition, Huisgen reaction, Heterogeneous catalysis, Triazole



## INTRODUCTION

Nanomaterials find vast application in catalysis, electronics, medicine, and sensors due to their novel properties that are different from those of the corresponding bulk materials.<sup>1–4</sup> Nanocatalysts have high surface to volume ratio, and their surface atoms are very active relative to those of bulk catalysts.<sup>4–11</sup> In the regiospecific alkyne–azide cycloaddition reaction, copper(I) compounds are very often used for the activation of the alkyne substrate. These copper-catalyzed reactions have some serious problems because of the instability of simple copper(I) salts. The active species are often generated in situ from copper(II) salts, and for such reactions, it is necessary to use an additive, a cofactor, and a reducing agent.<sup>12</sup> The CuI/NR<sub>3</sub> system is not successful in aqueous or protic solvents. Besides, they require a large amount of catalyst (up to 2 equiv) and additive (up to 20 equiv). The cycloaddition proceeds very slowly even at elevated temperature with a prolonged reaction time (80–120 °C for 12–24 h) in many cases.<sup>13–16</sup> Tetraalkylammonium hydroxides can be used in the place of transition metal catalysts, but the formation of 4-triazenyl triazole as a byproduct is a problem in this case.<sup>17</sup> The metal catalyst is lost at the end in many homogeneous reactions and hence cannot be retraced and recycled. Several copper complexes have also been employed as catalysts, but the preparation of ligands in these cases involves the use of toxic and volatile organic solvents like THF, dichloroethane, toluene, acetonitrile, benzene, and divinylbenzene, consuming considerable time (6–18 h).<sup>18–21</sup>

Heterogeneous catalytic systems, on the other hand, can have advantages such as simpler isolation of the reaction products and recycling of the catalyst systems by filtration. Cu(I) species immobilized onto various supports such as silica,<sup>22</sup> zeolites,<sup>23</sup>

activated charcoal,<sup>24</sup> and titanium dioxide<sup>25</sup> have been reported recently. However, heterogeneous catalysts immobilized with Cu(I) species frequently suffer from the general thermodynamic instability of Cu(I), which results in its easy oxidation to Cu(II) and/or disproportionation to Cu(0) and Cu(II). Consequently, usage of copper(I) catalysts require an inert atmosphere and anhydrous solvents. Copper-catalyzed 1,3-dipolar cycloaddition in water may not be effective due to the strong coordination capacity of copper with water, and use of toxic organic solvents is unavoidable.<sup>25</sup>

Effective non-copper catalysts are not very popular toward the cycloaddition of alkynes and azides in aqueous medium. For instance, charcoal impregnated with a zinc and ruthenium hydride complex, RuH<sub>2</sub>(CO)-(PPh<sub>3</sub>)<sub>3</sub>, is described as an effective catalyst for the cycloaddition yielding 1,4-disubstituted 1,2,3-triazoles in DMF and benzene or THF as solvent, but the yield was not encouraging when water was tried as the solvent.<sup>26,27</sup> Recently, many articles and reviews highlight the catalytic use of nanoparticles suspended in colloidal solutions as well as those adsorbed in different supports like various metal oxides for organic transformations.<sup>1,9–11</sup> It is also found that gold nanoparticles are highly reactive when they are supported on metal oxides, and titania has been found to be the best support for gold nanoparticles to affect many chemical transformations.<sup>28–31</sup> The catalytic activity of gold has been established despite the belief that gold is devoid of any activity.<sup>32,33</sup> Gold catalysts can be considered one of the most powerful activators of C–C multiple bonds, which allows the

Received: May 17, 2013

Revised: July 18, 2013

Published: August 7, 2013

formation of C–C, C–O, C–N, and C–S bonds by nucleophilic attack on the reactive multiple bonds.<sup>34,35</sup> The use of water as solvent in organic transformations has many advantages: uncommon reactivities and selectivities, easy workup, mild reaction conditions, and enabling recycling of the catalyst.<sup>36–38</sup> In continuation of our search on green protocols for organic synthesis,<sup>39–41</sup> porous titania nanosphere-supported gold nanoparticles (abbreviated hereafter as Au/TiO<sub>2</sub>) have been promoted as a catalyst for the Huisgen [3 + 2] cycloaddition of azides and alkynes in the present investigation. A new library of triazoles has been generated. The reaction was attempted in aqueous medium, and the results are presented in this article.

## EXPERIMENTAL SECTION

**Materials.** Titanium *tetra*isopropoxide (Fluka, 99%) was used as the starting material for the preparation of porous titanium dioxide nanospheres, and chloroauric acid trihydrate (Sigma-Aldrich) was used as a precursor to prepare gold-loaded porous titanium dioxide (Au/TiO<sub>2</sub>) nanospheres.

**Preparation of Porous Titanium Dioxide Nanospheres.** Porous titanium dioxide nanospheres were prepared by a solvothermal method reported earlier.<sup>42</sup> Titanium *tetra*isopropoxide (10 mL) (Fluka, 99%) was added dropwise to 35 mL of distilled ethanol with constant stirring wherein a milky suspension was formed immediately. Five milliliters of double distilled water was then added drop by drop to the suspension. After 2 h of stirring, the whole suspension was transferred into a Teflon beaker and kept in a stainless steel autoclave at 115 °C for 12 h. The resulting white porous titanium dioxide nanospheres were separated through filtration and washed several times with double distilled water, dried at 100 °C for removal of water, and finally calcined at 400 °C for 3 h.

**Preparation of Porous Au/TiO<sub>2</sub> Nanospheres.** The porous Au/TiO<sub>2</sub> nanospheres were prepared through the deposition–precipitation method.<sup>43</sup> Accordingly, 100 mL of an aqueous solution of HAuCl<sub>4</sub>·3H<sub>2</sub>O (1.02 mM) was heated to 80 °C, and the pH was adjusted to 7 by dropwise addition of sodium hydroxide (1 M). Afterward, 1 g of porous titanium dioxide nanospheres were dispersed in the above solution followed by readjusting the pH to 7 with sodium hydroxide (0.2 M). The suspension was then heated at 80 °C (in oil bath) for 2 h with vigorous stirring. The solids were gathered by centrifugation (12,000 rpm for 10 min), washed five times by stirring in hot (50 °C) distilled water, and then centrifuged. After drying the samples under vacuum at 100 °C for 2 h, they were calcined at 350 °C for 2 h to get the porous Au/TiO<sub>2</sub> nanospheres.

**Characterization Techniques.** The crystal phases of the prepared nanospheres were investigated by using the X-ray diffraction analysis (Rigaku diffractometer, Cu K $\alpha$  radiation, 0.02° s<sup>-1</sup>). Particle size and contour of the prepared nanocatalysts were analyzed using a Quanta 200 FEG scanning electron microscope and TECNAI G2 modal transmission electron microscope. The surface area, pore volume, and pore diameter of the sample were measured with the assistance of a Micrometrics ASAP-2020 physisorption analyzer. Diffuse reflectance spectra (DRS) of the samples were recorded using a Shimadzu UV–vis 2550 spectrophotometer fitted with an ISR-2200 DRS accessory. HPLC analysis was carried out using a Shimadzu LC-6AD HPLC system employing 80:20 methanol–water as the mobile phase at 0.4 mL per min flow rate.

**Procedure for Preparation of Azide (2).**<sup>44,45</sup> To substituted phenacyl bromide/alkyl halide dissolved in acetone, sodium azide was added in a 1:1.5 molar ratio with drops of water and stirred for 10–15 min at room temperature. After completion of the reaction, the reaction mass was quenched with water. The solidified azide was filtered and dried. In the case of liquid azides, the reaction mixture was extracted with dichloromethane and dried over anhydrous sodium sulfate.

**Typical Procedure for Synthesis of Ethyl 1-(2-Oxo-2-arylethyl)-1H-1,2,3-triazole-4-carboxylate (3).** To a mixture of

ethyl propiolate (0.72 mmol) and substituted phenacyl azide (0.6 mmol) in distilled water (10 mL), porous Au/TiO<sub>2</sub> nanospheres (2 mg) were added at room temperature. The reaction mixture was heated in a water bath for 30 min. After the completion of the reaction, the reaction mixture was cooled to room temperature. Then the product was extracted with a minimum amount of chloroform and dried over sodium sulfate. The product was crystallized in a chloroform–ethyl acetate mixture (3:2) to yield pure ethyl 1-(2-oxo-2-arylethyl)-1H-1,2,3-triazole-4-carboxylate (3) as a crystalline solid. For the time–conversion studies, 200  $\mu$ L of reaction mixture was withdrawn at regular time intervals and dissolved in 1.8 mL of DCM from which 100  $\mu$ L was injected to the HPLC column.

## RESULTS AND DISCUSSION

**X-ray Diffraction Analysis of TiO<sub>2</sub> and Au/TiO<sub>2</sub> Nanospheres.** The XRD patterns of porous TiO<sub>2</sub> and Au/TiO<sub>2</sub> nanospheres are shown in Figure 1. The X-ray diffraction

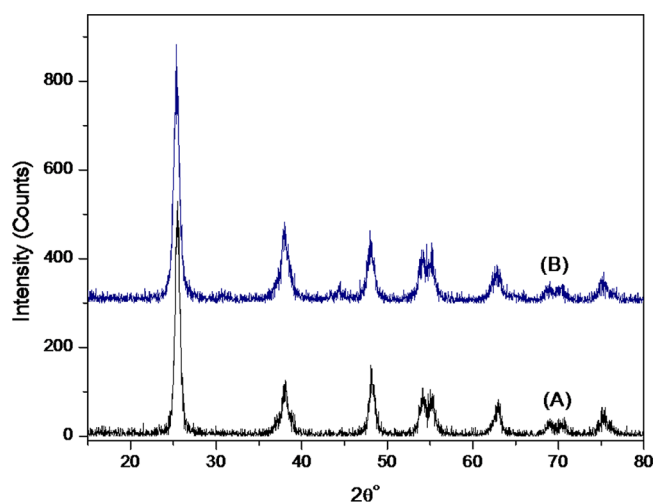


**Figure 1.** XRD patterns of porous TiO<sub>2</sub> (A) and Au/TiO<sub>2</sub> (B) nanospheres.

peaks observed at  $2\theta$  values of 25.46, 37.88, 48.06, 53.94, 55.11, 62.86, and 75.10° correspond to the (1 0 1), (0 0 4), (2 0 0), (1 0 5), (2 1 1), (2 0 4), and (2 1 5) plans of the anatase phase of TiO<sub>2</sub> [JCPDS file no. 11272]. This reveals that porous TiO<sub>2</sub> nanospheres have a single phase of anatase. Furthermore, the porous Au/TiO<sub>2</sub> nanospheres exhibit a peak at 44° corresponding to the (2 0 0) plane of Au crystal lattice. The peak resulting from (1 1 1) planes (38°) of Au might have been buried in the anatase peak at 37.88°. These peaks were emphasized for crystal lattices of Au in the form of a face-centered cubic (*fcc*) crystal system [JCPDS file no. 40784]. Besides, the  $2\theta$  values at which the major peaks appear are found to be almost the same for both TiO<sub>2</sub> and Au/TiO<sub>2</sub>, indicating that the porous TiO<sub>2</sub> crystal structure was not altered while doping with Au nanoparticles.

**SEM, HRTEM, and EDAX Analyses of TiO<sub>2</sub> and Au/TiO<sub>2</sub> Nanospheres.** Figure 2(A) shows the SEM image of the porous TiO<sub>2</sub> nanospheres revealing the nanospheres average diameter to be about 150 nm. The high magnification SEM image shows that the porous TiO<sub>2</sub> nanospheres are composed of many TiO<sub>2</sub> nanoparticles of ~10 nm size (Figure 2(A) inset). The TEM image (Figure 2(B)) clearly exhibits the porous structures of the Au/TiO<sub>2</sub> nanospheres, formed by the assembly of TiO<sub>2</sub> nanoparticles of about 10 nm. The HRTEM image (Figure 2(C)) of the Au/TiO<sub>2</sub> nanospheres illustrates

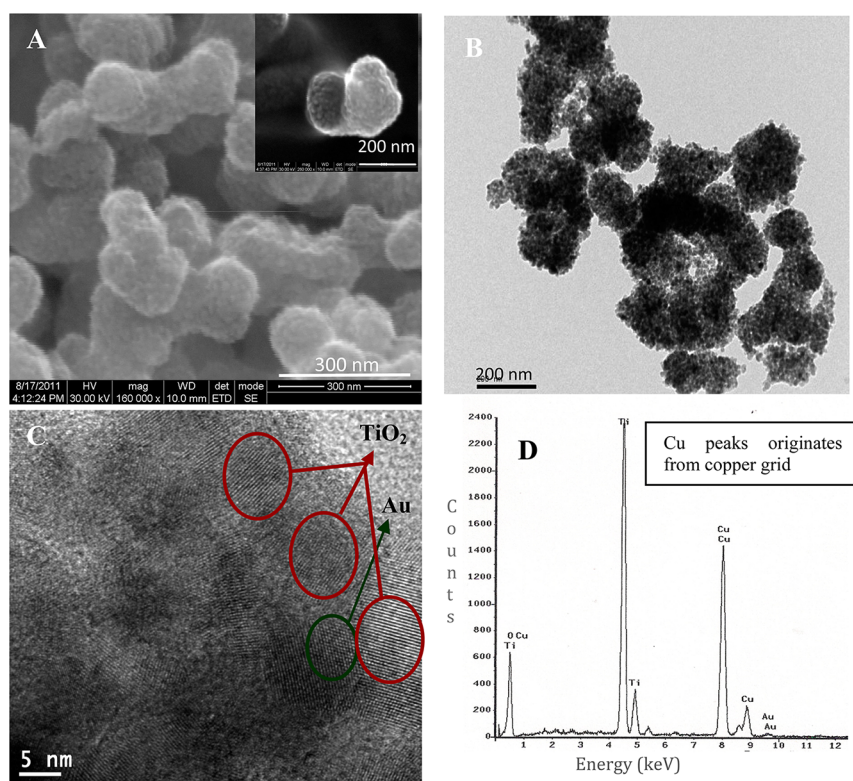


**Figure 2.** (A) SEM image of porous TiO<sub>2</sub>. Inset: Magnified image of a single TiO<sub>2</sub> nanosphere. (B) TEM image of Au/TiO<sub>2</sub>. (C) HRTEM image of Au/TiO<sub>2</sub>. (D) EDAX spectrum of porous Au/TiO<sub>2</sub>.

that Au nanoparticles with size of  $\sim 5$  nm are dispersed on the porous TiO<sub>2</sub> surface. The EDAX spectrum confirmed the presence of Au on the porous TiO<sub>2</sub> matrix (Figure 2(D)). In the EDAX spectrum, the peak due to Cu originates from the Cu grid used. The HRTEM image also clearly shows the polycrystalline nature of a single Au/TiO<sub>2</sub> nanosphere, which was further confirmed from the continuous sharp circles formed in the selected area electron diffraction (SAED) pattern.

**Nitrogen Adsorption–desorption Analysis of Porous TiO<sub>2</sub> and Au/TiO<sub>2</sub> Nanospheres.** The mesoporous structural characteristics of the obtained porous TiO<sub>2</sub> and Au/TiO<sub>2</sub> nanosphere were analyzed through N<sub>2</sub> adsorption–desorption experiments. Figure 3 exhibits the N<sub>2</sub> adsorption–desorption isotherms and their corresponding pore diameter distribution curves (inset) for the TiO<sub>2</sub> and Au/TiO<sub>2</sub> nanospheres. Well-defined adsorption steps in the relative pressure ( $P/P_0$ ) range of 0.6–0.84 and 0.6–0.8 were observed for the porous TiO<sub>2</sub> and Au/TiO<sub>2</sub>, respectively. The curves exhibited a type IV isotherm, a typical characteristic of mesoporous materials.<sup>46</sup> Moreover, the Barrett–Joyner–Halenda (BJH) pore size distribution plots (Figure 3, inset) reveal that the Au/TiO<sub>2</sub> nanospheres contain slightly smaller pore sizes and a narrower size distribution compared to those of TiO<sub>2</sub> nanospheres, which indicates that the Au nanoparticles are doped on the porous TiO<sub>2</sub> matrix. This is in good agreement with the TEM results. Furthermore, the BET specific surface area, pore volume, and pore size of TiO<sub>2</sub> nanospheres were found to be 104 m<sup>2</sup>/g, 0.29 cm<sup>3</sup>/g, and 3.7 nm, respectively, while those of the Au/TiO<sub>2</sub> nanospheres were 92 m<sup>2</sup>/g, 0.25 cm<sup>3</sup>/g, and 3.0 nm, respectively. As the Au/TiO<sub>2</sub> nanospheres possesses continuous particle framework together with high surface area and microporosity, these Au/TiO<sub>2</sub> nanospheres may offer large numbers of catalytic reaction centers that facilitate the

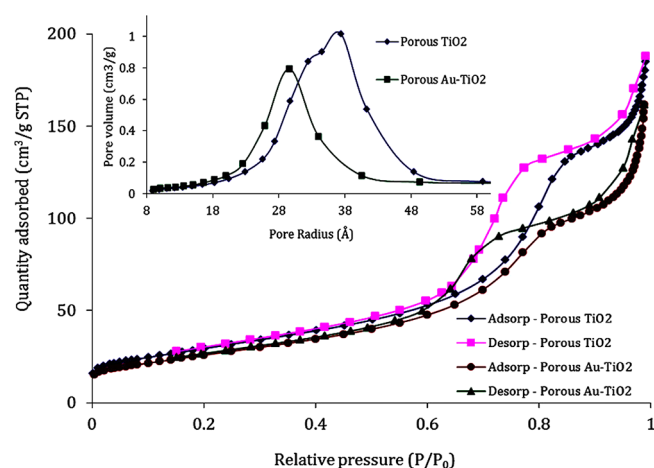


**Figure 3.** Nitrogen adsorption–desorption isotherms of porous TiO<sub>2</sub> and Au/TiO<sub>2</sub> nanospheres. Inset shows corresponding BJH pore size distribution plots.

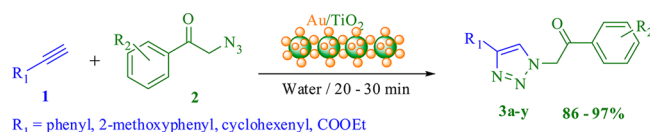
interaction between reactant molecules and the catalyst within the porous materials.

**UV–Vis Diffuse Reflectance and IR Spectral Analysis.** The diffused reflectance spectra and Tauc plots (inset) of porous TiO<sub>2</sub> and Au/TiO<sub>2</sub> nanospheres are shown in Figure S1 of the Supporting Information. As TiO<sub>2</sub> is an indirect transition semiconductor, plots of  $(\alpha h\nu)^{1/2}$  vs the energy ( $h\nu$ ) of absorbed light (Tauc plot) could be used to obtain the band gaps of the porous TiO<sub>2</sub> and Au/TiO<sub>2</sub> nanospheres. The extrapolation of the linear portion of the Tauc plots (Figure S1, inset, Supporting Information) give the band gap energy values of 3.07 and 3.08 eV for porous TiO<sub>2</sub> and Au/TiO<sub>2</sub> nanospheres, respectively, which indicates that the Au nano-

particles have not altered the band gap of the porous TiO<sub>2</sub> nanospheres. The appearance of a surface plasmon resonance band in the 520–620 nm range reveals the presence of Au nanoparticles on the porous TiO<sub>2</sub> matrix. Thus, these studies point out the presence of Au nanoparticles on the surface/pores of the TiO<sub>2</sub> nanospheres, which are in conformity with XRD and N<sub>2</sub>-adsorption studies.

**Synthesis of Triazoles Using Nanoporous Titania-Supported Gold Nanoparticles.** In a quest to develop efficient synthetic protocols, non-copper-catalyzed cycloaddition of alkyne with azide has been envisioned in this work. In a typical synthesis of triazoles, 0.6 mmol of phenacyl azides, 0.72 mmol of ethyl propiolate, and 2 mg of Au/TiO<sub>2</sub> were added in water and heated for 30 min in a water bath. After completion of the reaction, the product was obtained as a white solid (Scheme 1). To the best of our knowledge, this is the first report where Au/TiO<sub>2</sub> has been used to promote the regioselective synthesis of 1,4-disubstituted 1,2,3-triazoles in water.

#### Scheme 1. Titania-Supported Gold Nanosphere Catalyzed 1,2,3-Triazole Synthesis



The reaction of phenacyl azide with ethyl propiolate has been carried out in different solvents to choose the best solvent for this transformation. It is noticed that solvents like THF, ethanol, and dimethyl sulfoxide gave relatively moderate yield, while the use of toluene, *p*-xylene, 1,2-dichloroethane, and acetonitrile led to poor yield for this reaction. It is found that the rate of this Huisgen [3 + 2] cycloaddition has been accelerated in water or a *t*-BuOH/water mixture (Table S1, Supporting Information) ending up in excellent yield of 1,4-disubstituted 1,2,3-triazoles as a single regioisomer. Compared with organic solvents, water molecules can be adsorbed well on the surface of TiO<sub>2</sub>, and we believe that the better contact of the reactants in the aqueous medium with Au nanoparticles may have facilitated the reaction. A simple workup procedure without the need for chromatographic separation is the added advantage of this protocol. The recycled catalyst was thoroughly washed with dichloromethane and recycled five times without any significant loss in yield at a 30 min reaction time, and the details are presented in Figure S2 of the Supporting Information. It is tentatively believed that the catalytic activity has not been substantially decreased, and the decrease in yield could be due to the loss of the catalyst.

FT-IR spectra of porous TiO<sub>2</sub>, Au/TiO<sub>2</sub> nanospheres, and Au/TiO<sub>2</sub> recovered after reaction (for reuse) were recorded in the region 4000–400 cm<sup>-1</sup>. Both Au/TiO<sub>2</sub> and Au/TiO<sub>2</sub> recovered after the reaction show identical IR absorption bands indicating retainment of originality of the catalyst after the reaction. The recovered catalyst did not show any IR bands corresponding to the organic materials suggesting that the catalyst is not poisoned during the reaction (Figure S3, Supporting Information). An increase in the amount of catalyst from 2 to 20 mg decreased the time taken for completion of the reaction considerably (Figure 4). In a typical case (synthesis of 3a), the reaction was completed within 15 min in the presence of 20 mg of Au/TiO<sub>2</sub>, while it took 30 min for completion with

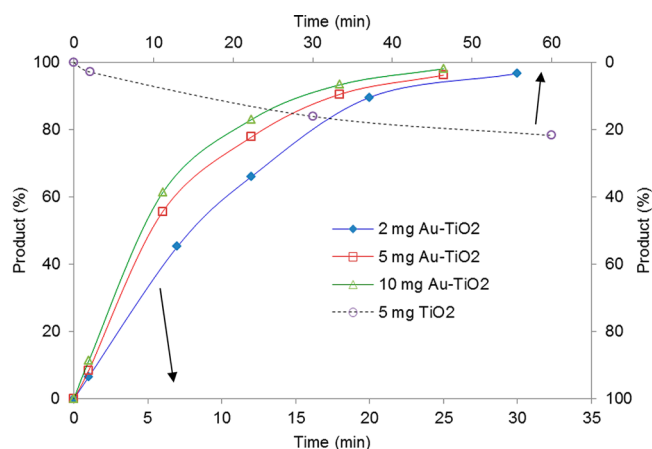


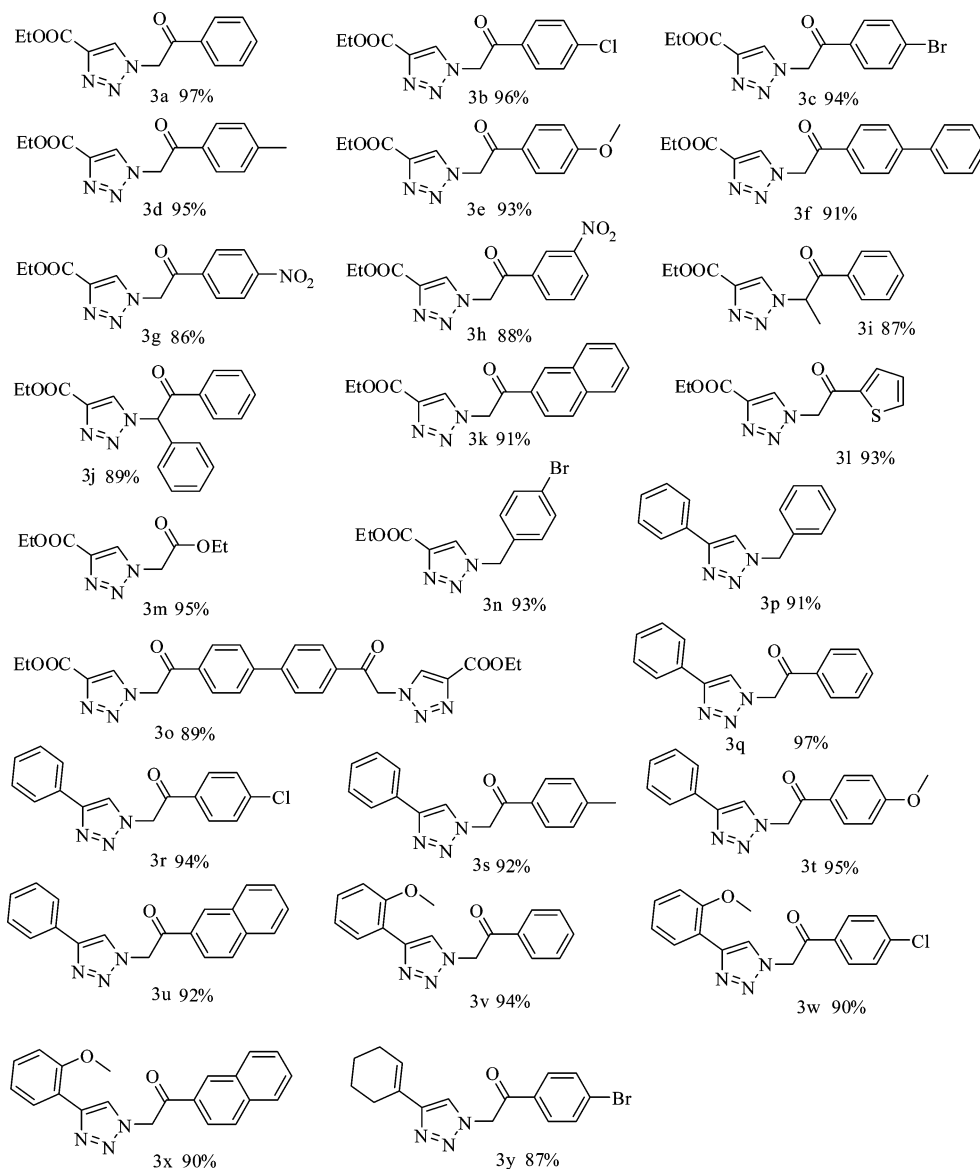
**Figure 4.** Time conversion of product 3a at various catalyst concentrations. The results of the reaction with TiO<sub>2</sub> only are plotted in the secondary (top and right) X and Y axes, while the results of the reactions with Au/TiO<sub>2</sub> are plotted in the primary (bottom and left) X and Y axes.

2 mg of Au/TiO<sub>2</sub> catalyst. Even though the reaction time was reduced to half when the amount of catalyst was increased by 10 times from the initial catalyst load, considering the cost of the catalyst, the reaction conditions were optimized with 2 mg of the catalyst. In the absence of Au/TiO<sub>2</sub> or in the presence of porous titania alone, the yield of 3a at a 30 min reaction time was poor (<20%). The representative high pressure liquid chromatograms obtained for the reaction mixture withdrawn at various time intervals is shown in Figure S4 of the Supporting Information. This reveals that the reaction is catalyzed by gold nanoparticles, which may help to enhance the electrophilicity of the alkyne.

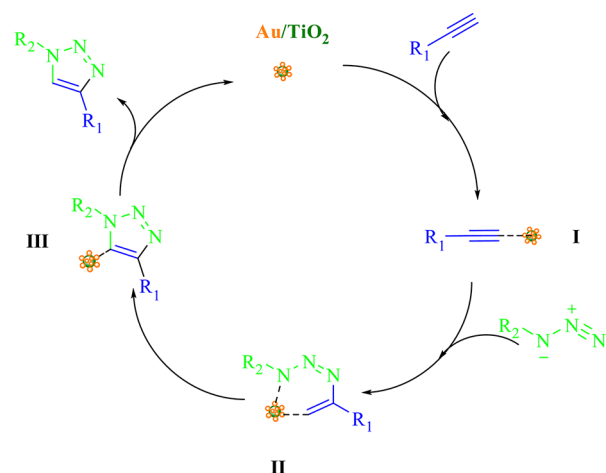
To evaluate the scope of this new Au/TiO<sub>2</sub> catalyzed process further, reactions of phenacyl azide with aliphatic and aromatic terminal alkynes substituted by electron donating as well as electron withdrawing groups were carried out. Likewise, the reactivity of alkynes with alkyl and aryl azides was also studied. Thus, a new triazole library has been created (3a–y; Table 1), and in all the cases, very good yields of a single regioisomer, namely 1,4-disubstituted 1,2,3-triazoles, were obtained. All the synthesized triazoles have been characterized through NMR spectral techniques (Figure S5–S56, Supporting Information).

On the basis of an analogy with previous reports,<sup>47</sup> a stepwise mechanism of cycloaddition is outlined in Scheme 2. In the proposed mechanism, the electron density of the alkyne is reduced by the gold atom (I) enabling that to undergo facile nucleophilic attack by azide.<sup>48,49</sup> The formation of a six member intermediate II can be proposed before getting the other intermediate III. Finally, removal of gold affords 1,4-disubstituted 1,2,3-triazoles as product (Scheme 2).

We have also tested the feasibility of conducting one-pot, three component, regioselective synthesis of 1,2,3-triazole from phenacyl/alkyl bromide, azide, and alkyne in the presence of a Au/TiO<sub>2</sub> catalyst. Here too, the corresponding 1,2,3-triazole is obtained (in 75% yield at 30 min) as a single regioisomer (Scheme S1, Supporting Information). However, as the crude reaction mixture was always contaminated with starting materials (in the three component system), the stepwise method is more advantageous than the three component reaction. Though the HMBC spectrum helps to arrive at the regiochemistry of 3, the regiochemistry has been unambiguously ascertained by the crystal structures (Figure S57,

Table 1. Synthesis of 1,2,3-Triazoles (3a–y) Using Nanoporous Au/TiO<sub>2</sub>

Scheme 2. Plausible Mechanism for the Formation of Triazole



Supporting Information) of 3a, 3c, and 3d, and the crystal data have been submitted to CCDC (CCDC-890748 to 890750).

We have also examined the efficiency of the Au/TiO<sub>2</sub> catalyst in the reaction of non-terminal alkynes with azide. It was found that the reaction of non-terminal alkyne with azide takes a relatively long time (>1.5 h) in the absence of the catalyst, which leads to an incomplete reaction. But interestingly, in the presence of the catalyst, the cycloaddition was completed in a short time (45 min) with good to excellent yield (4a–g, Scheme 3, Table 2). This may be due to the alkynophilic (not oxophilic) nature of gold, which may activate the non-terminal alkyne and improve the rate of reaction. All the synthesized triazoles have been characterized through NMR spectral techniques (Figure S58–S71, Supporting Information).

In reactions involving other nanocatalysts for triazole synthesis under aqueous medium, the catalyst load used was higher than Au/TiO<sub>2</sub> employed in our case, and also those reactions required prolonged heating.<sup>50–54</sup> Because of thermodynamical instability, recovered nanocopper loses its catalytic efficiency in water. In contrast, supported gold has sufficient stability in water. Also, due to the small size and

Scheme 3. Reaction of Azide with Non-Terminal Alkynes

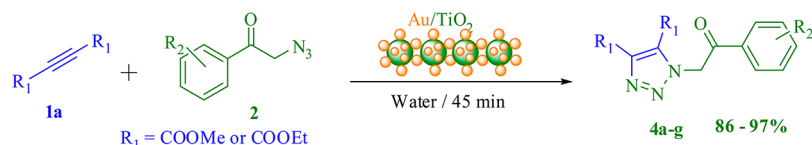
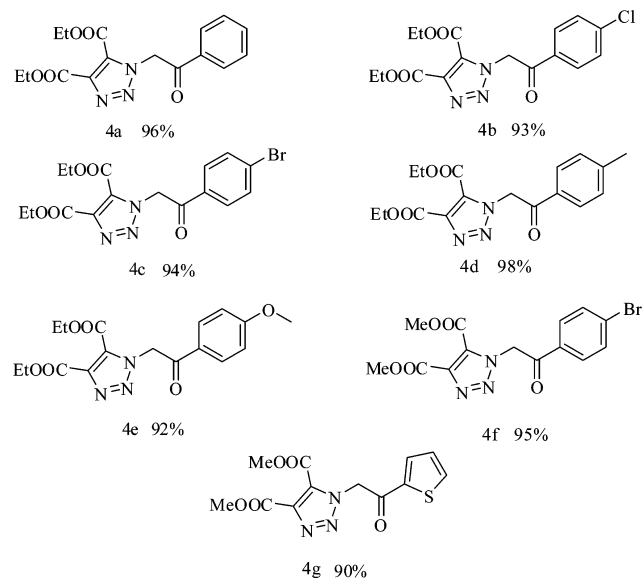


Table 2. Rate-Enhanced Synthesis of Triazoles from Non-Terminal Alkynes



nanoporous nature of Au/TiO<sub>2</sub> nanoparticles, a large surface area for effective cycloaddition is available. It can be recovered and reused up to five times without any significant loss of product yield at a given reaction time.

## CONCLUSION

In conclusion, porous TiO<sub>2</sub> nanospheres of about 150 nm in diameter have been prepared using the solvo-thermal method and were utilized for the preparation of porous Au/TiO<sub>2</sub> nanospheres through the deposition–precipitation method. It is reported for the first time that Au/TiO<sub>2</sub> can serve as an active catalyst in the Huisgen [3 + 2] cycloaddition of azides with terminal alkynes in aqueous medium, yielding 1,4-disubstituted 1,2,3-triazoles regioselectively as the sole product.

## ASSOCIATED CONTENT

### Supporting Information

Figures, table, scheme, and analytical data of the triazoles, <sup>1</sup>H and <sup>13</sup>C NMR spectra, and crystal data (Figure S1–S71, Table S1, and Scheme S1). This material is available free of charge via the Internet at <http://pubs.acs.org>.

## AUTHOR INFORMATION

### Corresponding Author

\*Tel.: (+91) 0452-2458246. Fax 0452-2459845. E-mail: [muthumanian2001@yahoo.com](mailto:muthumanian2001@yahoo.com).

### Notes

The authors declare no competing financial interest.

## ACKNOWLEDGMENTS

The authors thank DST, New Delhi, for assistance under the IRHPA program for the NMR facility. Financial support from

UGC, New Delhi, to Mr. M. Boominathan and from CSIR, New Delhi, to Mr. N. Pugazhenthiran are gratefully acknowledged.

## REFERENCES

- Polshettiwar, V.; Varma, R. S. Green chemistry by nano-catalysis. *Green Chem.* **2010**, *12*, 743–754.
- Rao, C. N. R.; Muller, A.; Cheetham, A. K. *Nanomaterials Chemistry: Recent Developments and New Directions*; Wiley-VCH: Weinheim, Germany, 2007; ISBN: 3527316647.
- Laurent, S.; Forge, D.; Port, M.; Roch, A.; Robic, C.; Elst, L. V.; Muller, R. N. Magnetic iron oxide nanoparticles: Synthesis, stabilization, vectorization, physicochemical characterizations, and biological applications. *Chem. Rev.* **2008**, *108*, 2064–2110.
- Burda, C.; Chen, Z.; Narayanan, R.; El-sayed, M. A. Chemistry and properties of nanocrystals of different shapes. *Chem. Rev.* **2005**, *105*, 1025–1102.
- Narayanan, R.; El-Sayed, M. A. Catalysis with transition metal nanoparticles in colloidal solution: Nanoparticle shape dependence and stability. *J. Phys. Chem. B.* **2005**, *109*, 12663–12676.
- Coperet, C.; Chabanas, M.; Saint-Arroman, R. P.; Basset, J. M. Homogeneous and heterogeneous catalysis: Bridging the gap through surface organometallic chemistry. *Angew. Chem., Int. Ed.* **2003**, *42*, 156–181.
- Basset, J. M.; Choplin, A. Surface organometallic chemistry: A new approach to heterogeneous Catalysis? *J. Mol. Catal.* **1993**, *21*, 95–108.
- Mizuno, N.; Misono, M. Heterogeneous catalysis. *Chem. Rev.* **1998**, *98*, 199–218.
- Polshettiwar, V.; Len, C.; Fihri, A. Silica-supported palladium: Sustainable catalysts for cross-coupling reactions. *Coord. Chem. Rev.* **2009**, *253*, 2599–2626.
- Shi, F.; Tse, M. K.; Zhou, S.; Pohl, M. M.; Radnik, J.; Hubner, S.; Jahnsch, K.; Bruckner, A.; Beller, M. Green and efficient synthesis of sulfonamides catalyzed by nano-Ru/Fe<sub>3</sub>. *J. Am. Chem. Soc.* **2009**, *131*, 1775–1779.
- Polshettiwar, V.; Baruwati, B.; Varma, R. S. Nanoparticle-supported and magnetically recoverable nickel catalyst: A robust and economic hydrogenation and transfer hydrogenation protocol. *Green Chem.* **2009**, *11*, 127–131.
- Lal, S.; Díez-Gonzalez, S. [CuBr(PPh<sub>3</sub>)<sub>3</sub>] for azide–alkyne cycloaddition reactions under strict click conditions. *J. Org. Chem.* **2011**, *76*, 2367–2373.
- Jagasia, R.; Holub, J. M.; Bollinger, M.; Kirshenbaum, K.; Finn, M. G. Peptide cyclization and cyclodimerization by Cu<sup>I</sup>-mediated azide–alkyne cycloaddition. *J. Org. Chem.* **2009**, *74*, 2964–2974.
- Luo, S.; Xu, H.; Mi, X.; Li, J.; Zheng, X.; Cheng, J.-P. Evolution of pyrrolidine-type asymmetric organocatalysts by “click” chemistry. *J. Org. Chem.* **2006**, *71*, 9244–9247.
- Nahrwold, M.; Bogner, T.; Eissler, S.; Verma, S.; Sewald, N. Clicktrophycin-52<sup>+</sup>: A bioactive cryptophycin-52 triazole analogue. *Org. Lett.* **2010**, *12*, 1064–1067.
- Shetti, V. S.; Ravikanth, M. Synthesis of triazole-bridged unsymmetrical porphyrin dyads and porphyrin–ferrocene conjugates. *Eur. J. Org. Chem.* **2010**, 494–508.
- Kwok, S. W.; Fotsing, J. R.; Fraser, R. J.; Rodionov, V. O.; Fokin, V. V. Transition-metal-free catalytic synthesis of 1,5-diaryl-1,2,3-triazoles. *Org. Lett.* **2010**, *12*, 4217–4219.

- (18) Nakamura, T.; Terashima, T.; Ogata, K.; Fukuzawa, S.-I. Copper(I) 1,2,3-triazol-5-ylidene complexes as efficient catalysts for click reactions of azides with alkynes. *Org. Lett.* **2011**, *13*, 620–623.
- (19) Liu, M.; Reiser, O. A copper(I) isonitrile complex as a heterogeneous catalyst for azide–alkyne cycloaddition in water. *Org. Lett.* **2011**, *13*, 1102–1105.
- (20) Ozcubukcu, S.; Ozkal, E.; Jimeno, C.; Pericas, M. A. A highly active catalyst for Huisgen 1,3-dipolar cycloadditions based on the tris(triazolyl)methanol–Cu(I) structure. *Org. Lett.* **2009**, *11*, 4680–4683.
- (21) Lal, S.; McNally, J.; White, A. J. P.; Díez-González, S. Novel phosphinite and phosphonite copper(I) complexes: Efficient catalysts for click azide–alkyne cycloaddition reactions. *Organometallics* **2011**, *30*, 6225–6232.
- (22) Miao, T.; Wang, L. Regioselective synthesis of 1,2,3-triazoles by use of a silica-supported copper(I) catalyst. *Synthesis* **2008**, 363–368.
- (23) Chassaing, S.; Sido, A. S. S.; Alix, A.; Kumarraja, M.; Pale, P.; Sommer, J. Click chemistry” in zeolites: Copper(I) zeolites as new heterogeneous and ligand-free catalysts for the Huisgen [3 + 2] cycloaddition. *Chem.—Eur. J.* **2008**, *14*, 6713–6721.
- (24) Lipshutz, B. H.; Taft, B. R. Heterogeneous copper-in-charcoal-catalyzed click chemistry. *Angew. Chem.* **2006**, *118*, 8415–8418.
- (25) Yamaguchi, K.; Oishi, T.; Katayama, T.; Mizuno, N. A supported copper hydroxide on titanium oxide as an efficient reusable heterogeneous catalyst for 1,3-dipolar cycloaddition of organic azides to terminal alkynes. *Chem.—Eur. J.* **2009**, *15*, 10464–10472.
- (26) Meng, X.; Xu, X.; Gao, T.; Chen, B. Zn/C-catalyzed cycloaddition of azides and aryl alkynes. *Eur. J. Org. Chem.* **2010**, 5409–5414.
- (27) Liu, P.-N.; Siyang, H.-X.; Zhang, L.; Tse, S. K. S.; Jia, G. RuH<sub>2</sub>(CO)(PPh<sub>3</sub>)<sub>3</sub> catalyzed selective formation of 1,4-disubstituted triazoles from cycloaddition of alkynes and organic azides. *J. Org. Chem.* **2012**, *77*, 5844–5849.
- (28) Corma, A.; Garcia, H. Supported gold nanoparticles as catalysts for organic reactions. *Chem. Soc. Rev.* **2008**, *37*, 2096–2126.
- (29) Mendez, V.; Caps, V.; Daniele, S. Design of hybrid titania nanocrystallites as supports for gold catalysts. *Chem. Commun.* **2009**, 3116–3118.
- (30) Kittisakmontree, P.; Pongthawornsakun, B.; Yoshida, H.; Fujita, S.; Arai, M.; Panpranot, J. The liquid-phase hydrogenation of 1-heptyne over Pd–Au/TiO<sub>2</sub> catalysts prepared by the combination of incipient wetness impregnation and deposition–precipitation. *J. Catal.* **2013**, *297*, 155–164.
- (31) Zanella, R.; Louis, C.; Giorgio, S.; Touroude, R. Crotonaldehyde hydrogenation by gold supported on TiO<sub>2</sub>: Structure sensitivity and mechanism. *J. Catal.* **2004**, *223*, 328–339.
- (32) Rudolph, M.; Hashmi, A. S. K. Gold catalysis in total synthesis—an update. *Chem. Soc. Rev.* **2012**, *41*, 2448–2462.
- (33) Brouwer, Z.; Li, C.; He, C. Gold-catalyzed organic transformations. *Chem. Rev.* **2008**, *108*, 3239–3265.
- (34) Corma, A.; Perez, A. L.; Sabater, M. J. Gold-catalyzed carbon–heteroatom bond-forming reactions. *Chem. Rev.* **2011**, *111*, 1657–1712.
- (35) Hashmi, A. S. K. Homogeneous gold catalysis beyond assumptions and proposals—characterized intermediates. *Angew. Chem., Int. Ed.* **2010**, *49*, 5232–5241.
- (36) Diebolt, O.; Muller, C.; Vogt, D. On-water” rhodium-catalyzed hydroformylation for the production of linear alcohols. *Catal. Sci. Technol.* **2012**, *2*, 773–777.
- (37) Lindstrom, U. M. Stereoselective organic reactions in water. *Chem. Rev.* **2002**, *102*, 2751–2772.
- (38) Li, P.; Wang, L. One-pot synthesis of 1,2,3-triazoles from benzyl and alkyl halides, sodium azide and alkynes in water under transition-metal-catalyst free reaction conditions. *Letters in Organic Chemistry* **2007**, *4*, 23–26.
- (39) Boominathan, M.; Nagaraj, M.; Muthusubramanian, S.; Krishnakumar, R. V. Efficient atom economical one-pot multi-component synthesis of densely functionalized 4H-chromene derivatives. *Tetrahedron* **2011**, *67*, 6057–6064.
- (40) Chitra, S.; Paul, N.; Muthusubramanian, S.; Manisankar, P. A facile, water mediated, microwave-assisted synthesis of 4,6-diaryl-2,3,3a,4-tetrahydro-1H-pyrido[3,2,1-jk]carbazoles by a domino Fischer indole reaction–intramolecular cyclization sequence. *Green Chem.* **2011**, *13*, 2777–2785.
- (41) Paul, N.; Kaladevi, S.; Muthusubramanian, S. Microwave-assisted stereoselective 1,3-dipolar cycloaddition of C,N-diarylnitrone (i.e., N-(arylmethylidene)benzenamine N-oxide) and bis-(arylmethylidene)acetone (=1,5-diarylpenta-1,4-dien-3-one): NMR and crystal analysis of diastereoisomeric bis(isoxazolines). *Helv. Chim. Acta* **2012**, *95*, 173–184.
- (42) Ahmmad, B.; Kusumoto, Y.; Islam, M. S. One-step and large scale synthesis of non-metal doped TiO<sub>2</sub> microspheres and their photocatalytic activity. *Adv. Powder Technol.* **2010**, *21*, 292–297.
- (43) Zanella, R.; Giorgio, S.; Shin, C. H.; Henry, C. R.; Louis, C. Characterization and reactivity in CO oxidation of gold nanoparticles supported on TiO<sub>2</sub> prepared by deposition-precipitation with NaOH and urea. *J. Catal.* **2004**, *222*, 357–367.
- (44) Moumne, R.; Larue, V.; Seijo, B.; Lecourt, T.; Micouin, L.; Tisne, C. Tether influence on the binding properties of tRNA<sup>Lys</sup><sub>3</sub> ligands designed by a fragment-based approach. *Org. Biomol. Chem.* **2010**, *8*, 1154–1159.
- (45) Santos, A.; El-Kaim, L.; Grimaud, L.; Ronsseray, C. Unconventional oxazole formation from isocyanides. *Chem. Commun.* **2009**, *0*, 3907–3909.
- (46) Guo, F. Q.; Li, H. F.; Zhang, Z. F.; Meng, S. L.; Li, D. Q. Synthesis of mesoporous YF<sub>3</sub> nanoflowers via solvent extraction route. *J. Mater. Sci. Eng. B* **2009**, *163*, 134–137.
- (47) Kidwai, M.; Bansal, V.; Kumar, A.; Mozumdar, S. The first Au-nanoparticles catalyzed green synthesis of propargylamines via a three-component coupling reaction of aldehyde, alkyne and amine. *Green Chem.* **2007**, *9*, 742–745.
- (48) Asao, N.; Nogami, T.; Lee, S.; Yamamoto, Y. Lewis acid-catalyzed benzannulation via unprecedented [4 + 2] cycloaddition of o-alkynyl(oxo)benzenes and enynals with alkynes. *J. Am. Chem. Soc.* **2003**, *125*, 10921–10925.
- (49) Asao, N.; Takahashi, K.; Lee, S.; Kasahara, T.; Yamamoto, Y. AuCl<sub>3</sub>-catalyzed benzannulation: Synthesis of naphthyl ketone derivatives from o-alkynylbenzaldehydes with alkynes. *J. Am. Chem. Soc.* **2002**, *124*, 12650–12651.
- (50) Borah, B. J.; Dutta, D.; Saikia, P. P.; Barua, N. C.; Dutta, D. K. Stabilization of Cu(0)-nanoparticles into the nanopores of modified montmorillonite: An implication on the catalytic approach for “click” reaction between azides and terminal alkynes. *Green Chem.* **2011**, *13*, 3453–3460.
- (51) Orgueira, H. A.; Fokas, D.; Isome, Y.; Chan, P. C.-M.; Baldino, C. M. Regioselective synthesis of [1,2,3]-triazoles catalyzed by Cu(I) generated in situ from Cu(0) nanosize activated powder and amine hydrochloride salts. *Tetrahedron. Lett.* **2005**, *46*, 2911–2914.
- (52) Kim, J. Y.; Park, J. C.; Kang, H.; Song, H.; Park, K. H. CuO hollow nanostructures catalyze [3 + 2] cycloaddition of azides with terminal alkynes. *Chem. Commun.* **2010**, *46*, 439–441.
- (53) Kantam, M. L.; Jaya, S. V.; Sreedhar, B.; Rao, M. M.; Choudary, B. M. Preparation of alumina supported copper nanoparticles and their application in the synthesis of 1,2,3-triazoles. *J. Mol. Catal. A: Chem.* **2006**, *256*, 273–277.
- (54) Kaboudin, B.; Abedi, Y.; Yokomatsu, T. One-pot Synthesis of 1,2,3-Triazoles from boronic acids in water using Cu (II)- $\beta$ -cyclodextrin complex as a nanocatalyst. *Org. Biomol. Chem.* **2012**, *10*, 4543–4548.